A STUDY OF A FIRST PERTURBATION SOLUTION TO THE EQUATIONS OF MOTION OF A FREELY FALLING MISSILE

A THESIS

Presented to

the Faculty of the Graduate Division

by

Benjamin Ronn

In Partial Fulfillment

of the Requirements for the Degree

Master of Science in Aeronautical Engineering

Georgia Institute of Technology

December 1961

"In presenting the dissertation as a partial fulfillment of the requirements for an advanced degree from the Georgia Institute of Technology, I agree that the Library of the Institution shall make it available for inspection and circulation in accordance with its regulations governing materials of this type. I agree that permission to copy from, or to publish from, this dissertation may be granted by the professor under whose direction it was written, or, in his absence, by the dean of the Graduate Division when such copying or publication is solely for scholarly purposes and does not involve financial gain. It is understood that any copying from, or publication of, this dissertation which involves potential financial gain will not be allowed without written permission.

9 &
12T

A STUDY OF A FIRST PERTURBATION

SOLUTION TO THE EQUATIONS OF

MOTION OF A FREELY FALLING MISSILE

Approved:

Arnold L. Ducoffe

Jakob Mandelker

Frank M. White, Jr.

Date Approved by Chairman:

April 15, 1962

ACKNOWLEDGMENTS

The author is deeply indebted to Dr. Arnold L. Ducoffe for his suggestion of the topic and his invaluable assistance through all phases of the study. Gratitude is also extended to Dr. Frank M. White for suggesting the perturbation method of approach and to both Dr. White and Dr. Jakob M. Mandelker for their critical review of the subject.

Sincere appreciation is extended to the Sandia Corporation for the technical help and financial aid which made this work possible.

TABLE OF CONTENTS

LIST OF TABLES

LIST OF FIGURES

LIST OF FIGURES (CONT.)

Figure | Page

LIST OF SYMBOLS

English

a	local speed of sound, feet per second
b_n	constants in a power series expansion
c	speed of sound, feet per second
C_D	aerodynamic drag coefficient based on missile frontal area
$\overline{C}_D$	ratio of C_D to minimum C_D
D	aerodynamic drag, pounds
E_n	constants in a power series expansion
$\vec{F}$	force, pounds
g	gravitational acceleration, 32.17 feet per second per second
h	initial altitude, feet
K	ballistic parameter of the missile, square feet per slug
m	mass of the missile, slugs
M	Mach number, ratio of missile velocity to local speed of sound
S	frontal area of missile, square feet
t	time, seconds
u	initial horizontal velocity, feet per second
V	total velocity of the missile, feet per second

LIST OF SYMBOLS (CONT.)

English

w	weight of the missile, pounds
x	range or horizontal coordinate of missile location, feet
y	altitude or vertical coordinate of missile location, feet

Greek

ρ	local density of atmosphere, slugs per cubic feet
θ	angle between the direction of flight and the horizontal axis

Subscripts

i	initial conditions
min	minimum quantity of the function
$n = 1, 2, 3 \ldots$	order of the perturbation
o	zero drag conditions
s	numerical integration solution on high speed digital computer
p	first perturbation solution

Superscripts

$'$	first derivative with respect to time
$''$	second derivative with respect to time

LIST OF SYMBOLS (CONT.)

Symbols

( )	term preceding this symbol is a function of the variable contained within these parentheses.

SUMMARY

A study was conducted to determine the feasibility of a first perturbation solution to the differential equations of motion of a freely falling missile as a method of obtaining rapid prediction of trajectories.

The following assumptions prevail in the derivation of the equations of motion:

1. The earth is flat, nonrotating and has a homogene ous gravity field.

2. The missile falls freely through standard atmosphere with ideal tractability and without spinning.

A numerical integrating method (Runge-Kutta) adaptable to high speed digital computers was used in Reference 1 to solve the following equations of motion:

$$x'' = K\bar{C}_D \rho \left[x'^2 + y'^2 \right]^{0.5} \left[x' \right]$$
$$y'' = K\bar{C}_D \rho \left[x'^2 + y'^2 \right]^{0.5} \left[y' \right] - g$$

Because of the complexity of the above equations of motion, a simpler set of equations which yields itself to rapid hand calculations was obtained. An approximate integration method (Simpson's Rule) adaptable to hand

calculators was used to solve the first perturbation solution of the equations of motion. The first perturbation expressions were obtained by expanding x, y, C_D and ρ in powers of K, in the equations of motion. The result was:

$$x_1'' = \rho\ (y_o)\overline{C}_D(M_o)V_o u$$

$$y_1'' = \rho\ (y_o)\overline{C}_D(M_o)V_o gt$$

A comparison of the above two methods of integration was performed by plotting $x_s - x_p$ and $y_s - y_p$ versus the ballistic parameter, K. Note that subscript, s, denotes the numerical integration solution on a high speed digital computer and, p, denotes the first perturbation solution.

The initial conditions used for this study were as follows:

1. Vertical velocity = zero in all cases.

2. Horizontal velocity = 400, 800 and 1,200 feet per second.

3. Altitude = 10, 50, 100 thousand feet.

The range of ballistic parameters used in this comparison was:

$$-0.035 \leq K \leq 0$$

An investigation of several missiles, i.e., Titan, Atlas, etc., indicated that the value of the ballistic parameter, K, of practical existing missiles fell in the range $-0.007 \leq K \leq 0$. Over this span of the ballistic parameter values the agreement between the results obtained by the two methods of integration was satisfactory.

The errors as indicated by the differences $x_s - x_p$ and $y_s - y_p$, using the range, x_s, and the altitude, y_s, of the trajectories computed by the digital computer as references, did not exceed five per cent.

The maximum errors appeared at large values of the ballistic parameter, $K < -0.007$, and large values of time, t, The errors reached values of over two hundred per cent at these conditions.

These results led to the conclusion that the perturbation solution to the equations of motion rendered itself as a practical field method to determine ballistic trajectories of freely falling realistic missiles.

CHAPTER I

INTRODUCTION

An earlier attempt to establish a field method of predicting trajectories of ballistic missiles was conducted by Hutchinson (Reference 1). The conclusions reached by Hutchinson, and further investigations of the data obtained from the digital computer, indicate the following:

1. Only when a specific trajectory (other than the zero drag trajectory) is known and only when the range of ballistic parameters on either side of the specific trajectory is very small, may a linear interpolation or extrapolation be used to determine another trajectory.

2. Interpolation along constant time lines was successful only for very small values of ballistic parameters.

Since the ultimate goal of obtaining a rapid method for determining trajectories was achieved only under restrictive conditions, an alternate approach, utilizing a first perturbation solution to the same equations of motion was undertaken. A first perturbation solution in conjunction with an approximate integration method was adapted to hand calculations requiring comparatively little time to perform on a slide rule or table calculator.

The purpose of this study is to evaluate the first perturbation solution as a method of rapidly predicting trajectories of ballistic missiles without the use of high speed digital computers. The evaluation is accomplished by comparing the trajectories obtained from two solutions to the equations of motion:

1. A numerical integration of the exact equations of motion on a high speed digital computer.

2. The first perturbation solution.

For the purpose of this study, the trajectories obtained by the first method are used as the acceptable reference. The trajectories of the second method are compared with the reference trajectories for the purpose of evaluating the perturbation solution as a field method.

CHAPTER II

THEORY

In the two dimensional study of the trajectories of a freely falling ballistic missile, the following assumptions are made:

1. The earth is flat, nonrotating and has a homogene ous gravity field.

2. The missile free falls through standard atmosphere with ideal tractability and without spinning.

3. The missile is assumed to be a point mass acted upon by the earth's gravitational forces and the aerodynamic drag force.

Newton's second law of motion is the starting point:

$$\vec{F} = m \frac{d\vec{V}}{dt} \qquad (1)$$

where $\vec{F}$ is the force vector, m, is the mass and, $\frac{d\vec{V}}{dt}$, is the acceleration vector.

Summation of forces acting upon the missile at any time, t, are shown in Figure 1 and the equations of force equilibrium are:

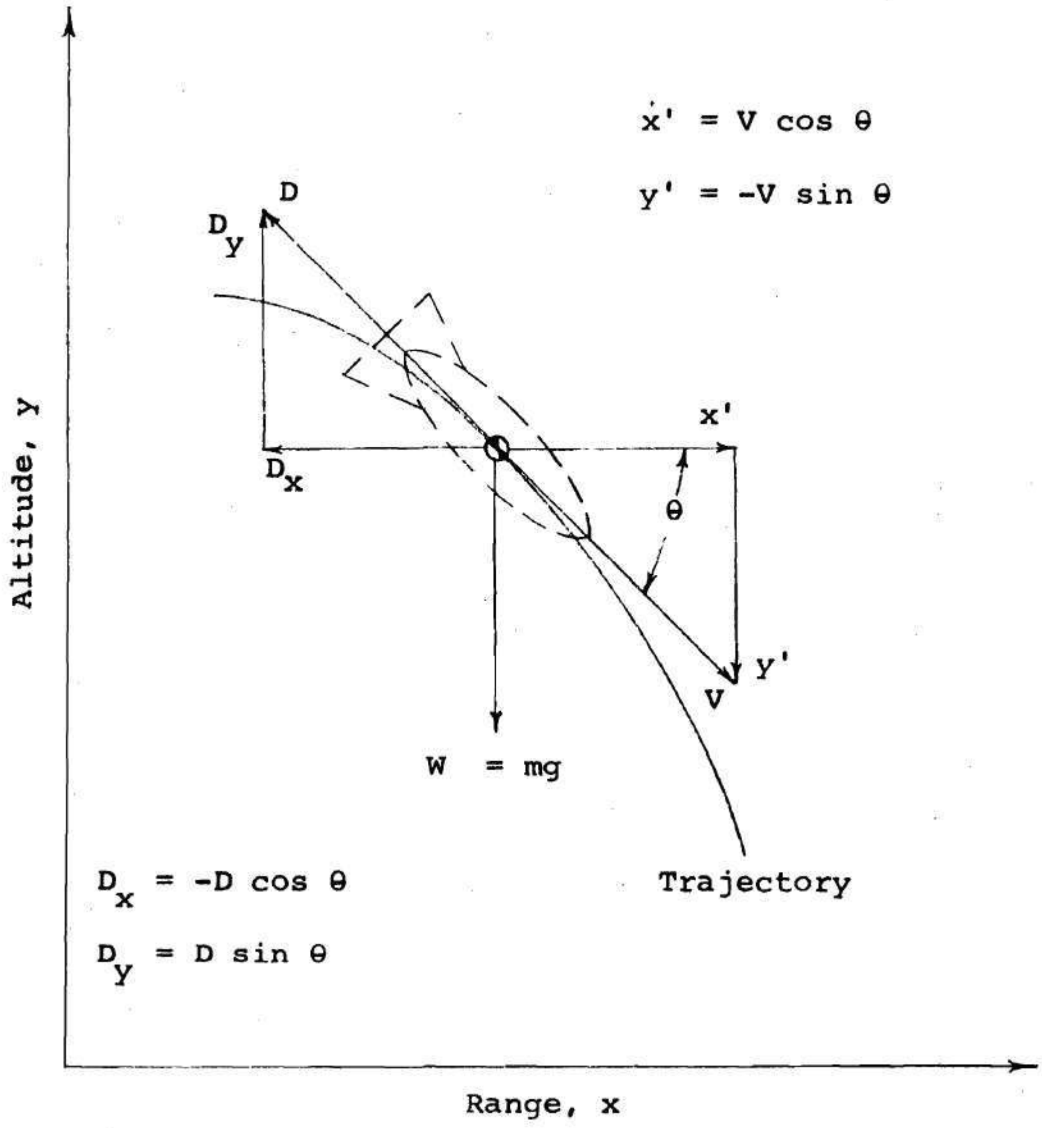

Figure 1. Sketch of the Dynamics of a Freely Falling Missile.

$$F_x = -D \cos \theta \tag{2}$$

$$F_y = D \sin \theta - mg \tag{3}$$

where F_x and F_y are the horizontal and vertical components, respectively, of the total force acting upon the missile, D is the drag force, θ is the angle between the direction of flight and the horizontal axis, and g is the gravitational acceleration.

Denote the accelerations in the horizontal and vertical directions as x" and y", respectively. Equation (1) in conjunction with Equations (2) and (3) can be written as:

$$x'' = -\left[D/m\right] \cos \theta \tag{4}$$

and

$$y'' = \left[D/m\right] \sin \theta - g \tag{5}$$

From the definition of drag coefficient, the drag can be written as:

$$D = \left[1/2\right] \rho V^2 S C_D \tag{6}$$

where ρ is density of the local atmosphere, V is the total missile velocity, S is the frontal area of the missile, and C_D is the aerodynamic drag coefficient.

By definition:

$$m = W/g \tag{7}$$

where W is the weight of the missile.

Substitution of Equations (6) and (7) into Equations (4) and (5) results in:

$$x'' = -\left[1/2\right] g\ C_D \left[S/W\right] \rho V^2 \cos\theta \tag{8}$$

and

$$y'' = \left[1/2\right] g\ C_D \left[S/W\right] \rho V^2 \sin\theta - g \tag{9}$$

The horizontal and vertical components of the velocity may be written as:

$$x' = V \cos\theta \tag{10}$$

and

$$y' = -V \sin\theta \tag{11}$$

The missile velocity is then expressed in terms of Equations (10) and (11) as:

$$V = \left[x'^2 + y'^2\right]^{0.5} \tag{12}$$

Substitution of Equations (10), (11) and (12) into Equations (8) and (9) yields:

$$x'' = \left[1/2\right] g\ C_D \left[S/W\right] \rho \left[x'^2 + y'^2\right]^{0.5} x' \tag{13}$$

$$y'' = -\left[1/2\right] g\ C_D \left[S/W\right] \rho \left[x'^2 + y'^2\right]^{0.5} y' - g \tag{14}$$

Define two parameters as follows:

$$\bar{C}_D = C_D / C_{D_{min}} \tag{15}$$

and

$$K = -\left[1/2\right] g \; C_{D_{min}} \left[\frac{1}{W/S}\right] \tag{16}$$

Note that $C_{D_{min}}$ is the value of the drag coefficient at Mach number $M = 0$ and K is the ballistic parameter. Substituting Equations (15) and (16) into Equations (13) and (14) gives:

$$x'' = K\bar{C}_D \, \rho\left[x'^2 + y'^2\right]^{0.5} x' \tag{17}$$

and

$$y'' = K\bar{C}_D \, \rho\left[x'^2 + y'^2\right]^{0.5} y' - g \tag{18}$$

Equations (17) and (18) are the non-linear equations of motion of the freely falling ballistic missile under consideration in this study.

The initial conditions in this study are:

$$x_{t=0} = 0 \qquad x'_{t=0} = u \tag{19}$$

$$y_{t=0} = h \qquad y'_{t=0} = 0$$

where h is the initial altitude and u is the initial horizontal velocity.

The Sandia Corporation of Albuquerque, New Mexico, provided the digital computer solutions of the equations of motion. These solutions were obtained by a numerical integration method (Runge-Kutta) adaptable to an IBM 704 high speed digital computer.

For the case of zero drag, i.e., $K = 0$, the differential equations of motion of an arbitrary mass can be written as:

$$x_o'' = 0 \tag{20}$$

and

$$y_o'' = -g \tag{21}$$

where subscript zero indicates zero drag conditions.

Double integration of Equations (20) and (21) and use of Equation (19) provides solutions of the form:

$$x_o = ut \tag{22}$$

$$y_o = h - \left[1/2\right]gt^2 \tag{23}$$

In order to arrive at a perturbation solution to the equations of motion, the following procedure was utilized:

Expand x and y in a power series in K about the zero drag trajectory.

The result is:

$$x = x_o + Kx_1 + K^2x_2 + \ldots + K^nx_n + \ldots \tag{24}$$

$$y = y_o + Ky_1 + K^2y_2 + \ldots + K^ny_n + \ldots \tag{25}$$

where n denotes the order of the perturbation.

Substitution of Equations (22) and (23) into Equations (24) and (25) yields:

$$x = ut + Kx_1 + K^2x_2 + \ldots \tag{26}$$

$$y = h - \left[1/2\right] gt^2 + Ky_1 + K^2y_2 + \ldots \tag{27}$$

Differentiating Equations (26) and (27) twice with respect to time and squaring the first derivative of each results in:

$$x' = u + Kx_1' + K^2x_2' + \ldots \tag{28}$$

$$x'^2 = u^2 + 2u\ Kx_1' + 2u\ K^2x_2' + \ldots \tag{29}$$

$$x'' = Kx_1'' + K^2x_2'' + \ldots \tag{30}$$

$$y' = -gt + Ky_1' + K^2y_2' + \ldots \tag{31}$$

$$y'^2 = g^2t^2 - 2gt\ Ky_1' - 2gt\ K^2y_2' + \ldots \tag{32}$$

$$y'' = -g + Ky_1'' + K^2y_2'' + \ldots \tag{33}$$

In Appendix A the density, ρ, and the speed of sound, a, are expanded in a power series of y, where y is expanded in a power series of K. The non-dimensional drag coefficient, $\overline{C_D}$, is expanded in a power series of Mach number, M, where M is expanded in a power series of K. The results of these expansions as derived in Appendix A are:

$$\rho = \rho_o + Ky_1 \frac{d\rho}{dy}(y_o) + K^2 y_2 \frac{d\rho}{dy}(y_o) + \ldots \tag{34}$$

$$a = a_o + Ky_1 \frac{da}{dy}(y_o) + K^2 y_2 \frac{da}{dy}(y_o) + \ldots \tag{35}$$

$$\overline{C}_D = \overline{C}_D(M_o) + K^2\left[2E_2M_oM_2 + 4E_4M_o^3M_2 + \ldots\right] + K^4\left[2E_2M_oM_4 + 4E_4M_o^3M_4 + \ldots\right] + \ldots \tag{36}$$

where the symbol ( ) denotes that the variable preceding the parentheses is a function of the variable within the parentheses and subscript zero denotes zero drag conditions.

The substitution of Equations (28) through (36) into Equations (17) and (18) is given in Appendix A. The results of these substitutions are:

$$x_1'' = K\overline{C}_D \frac{\left[u^2 + g^2t^2\right]^{0.5}}{a(y_o)} \rho(y_o)\left[u^2 + g^2t^2\right]^{0.5} u \tag{37}$$

and

$$y_1'' = -K\overline{C}_D \frac{\left[u^2 + g^2t^2\right]^{0.5}}{a(y_o)} \rho(y_o)\left[u^2 + g^2t^2\right]^{0.5} gt \tag{38}$$

where

$$\left[u^2 + g^2t^2\right]^{0.5} = V_o \tag{39}$$

is the total velocity of the freely falling missile at zero drag conditions.

From the definition in Appendix A, the Mach number at zero drag conditions can be expressed as:

$$M_o = \frac{V_o}{a_o} \tag{40}$$

Substituting Equations (39) and (40) into Equations (37) and (38) results in:

$$x_1'' = K\overline{C}_D(M_o)\rho(y_o)V_o u \tag{41}$$

$$y_1'' = -K\overline{C}_D(M_o)\rho(y_o)V_o gt \tag{42}$$

The right hand side of equations (41) and (42) is a function only of time. Successive integration of Equations (41) and (42) results in:

$$x_1' = \int_o^t \overline{C}_D(M_o)\rho(y_o)V_o u \, dt \tag{43}$$

$$x_1 = \int_o^t \int_o^z \overline{C}_D(M_o)\rho(y_o)V_o u \, dz \, dt \tag{44}$$

$$y_1' = -\int_o^t \overline{C}_D(M_o)\rho(y_o)V_o gt \, dt \tag{45}$$

$$y_1 = -\int_o^t \int_o^z \overline{C}_D(M_o)\rho(y_o)V_o gt \, dz \, dt \tag{46}$$

An approximate integration method (Simpson's Rule) is used to evaluate Equations (43) through (46). The non-dimensional drag coefficient, $\overline{C}_D$, curve as a function of Mach number, M, to be used in Equations (41) and (42) is shown in Figure 2.

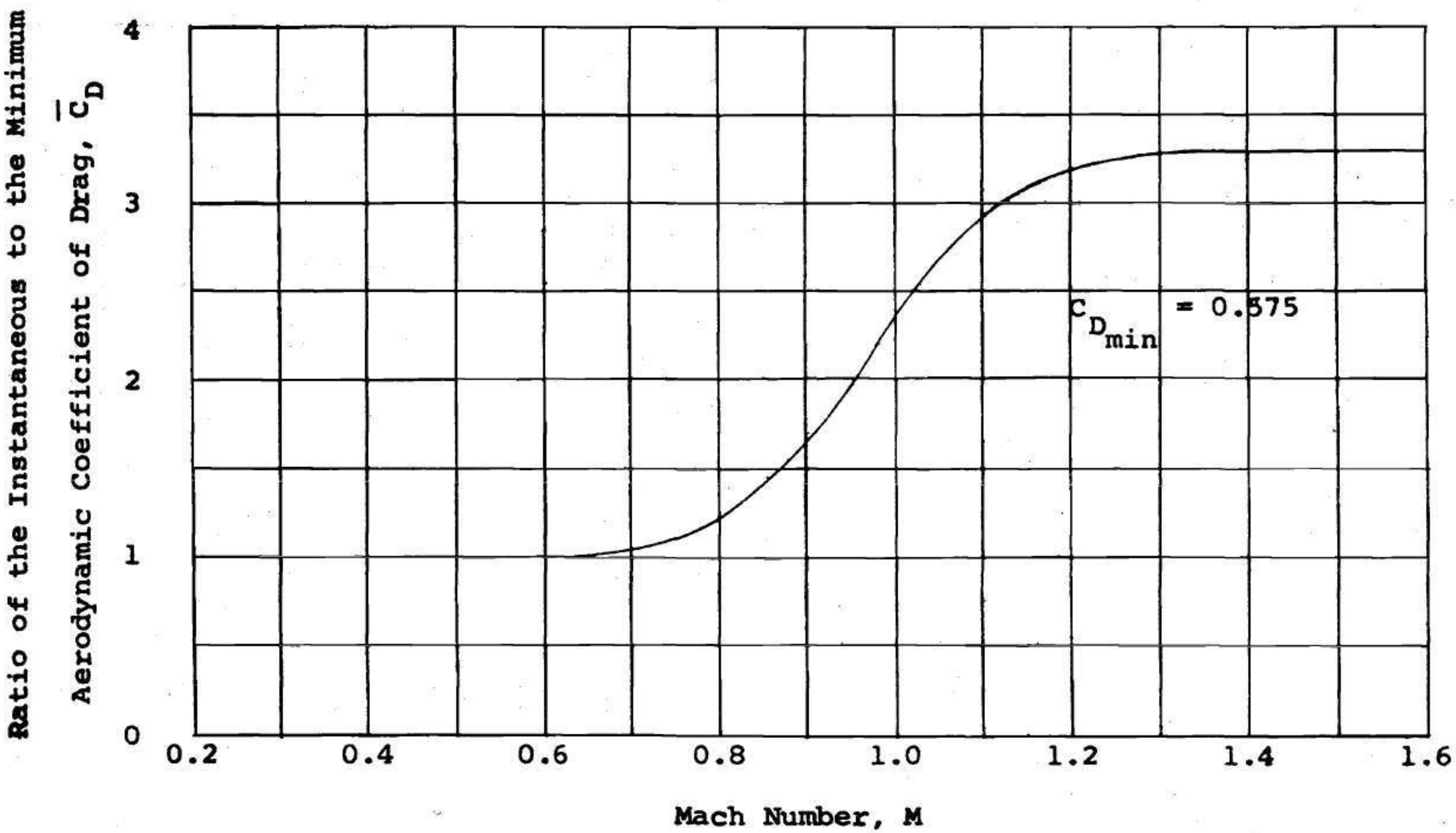

Figure 2. Non-Dimensional Drag Coefficient

Characteristics of the Missile in this Study.

CHAPTER III

METHODS OF SOLUTION

Reference Solution.--The solutions to Equations (17) and (18) were obtained from an IBM 704 digital computer using the Runge-Kutta method of integration. The solutions obtained represent all possible combinations of initial conditions and ballistic coefficients shown in Table 1.

All IBM 704 computed data was supplied by the Sandia Corporation of Albuquerque, New Mexico.

Perturbation Solution.--Solutions of the first perturbation equations of motion were obtained by using Simpson's Rule as an approximate integration method with time increments of two seconds.

The values of x_1 and y_1 obtained at each time interval were introduced into the basic perturbation Equations (26) and (27); the trajectories were then computed from the following relations:

$$x_p \approx x_o + Kx_1$$
$$y_p \approx y_o + Ky_1$$

where subscript p denotes the first perturbation solution.

Table 1. Initial Conditions and Ballistic Parameters Used in This Study

Initial Conditions		Ballistic Parameter
Altitude (Ft.)	Velocity (Ft./Sec.)	($Ft.^2$/Slug)
10,000	400	-0.007
50,000	800	-0.014
100,000	1,200	-0.021
		-0.028
		-0.035

Approximately three hours of calculations on an automatic hand calculator are required to generate a single trajectory, using a time increment of two seconds and an initial altitude of one hundred thousand feet or less.

CHAPTER IV

DISCUSSION OF RESULTS

A sketch of a zero drag trajectory, a reference trajectory, and a perturbation trajectory is presented in Figure 3. The validity of the perturbation solution to the equations of motion as a method of determining trajectories depends upon the correlation between the reference and the perturbation trajectories. In order to compare the results, the differences, $x_s - x_p$ and $y_s - y_p$, were plotted versus the ballistic parameters in Figures 4 through 17.

In Tables 2 through 4 the altitude, y_s, and the range, x_s, of the reference trajectories can be found for all initial conditions and ballistic parameters used in this study. These tables in conjunction with Figures 4 through 17 are used to determine differences or errors between the reference and perturbation trajectories in terms of altitude, y, and range, x.

Table 5 contains approximate values of the ballistic parameters for existing missiles. The Titan and Atlas, for instance, have K values of -0.0005. Other rockets and

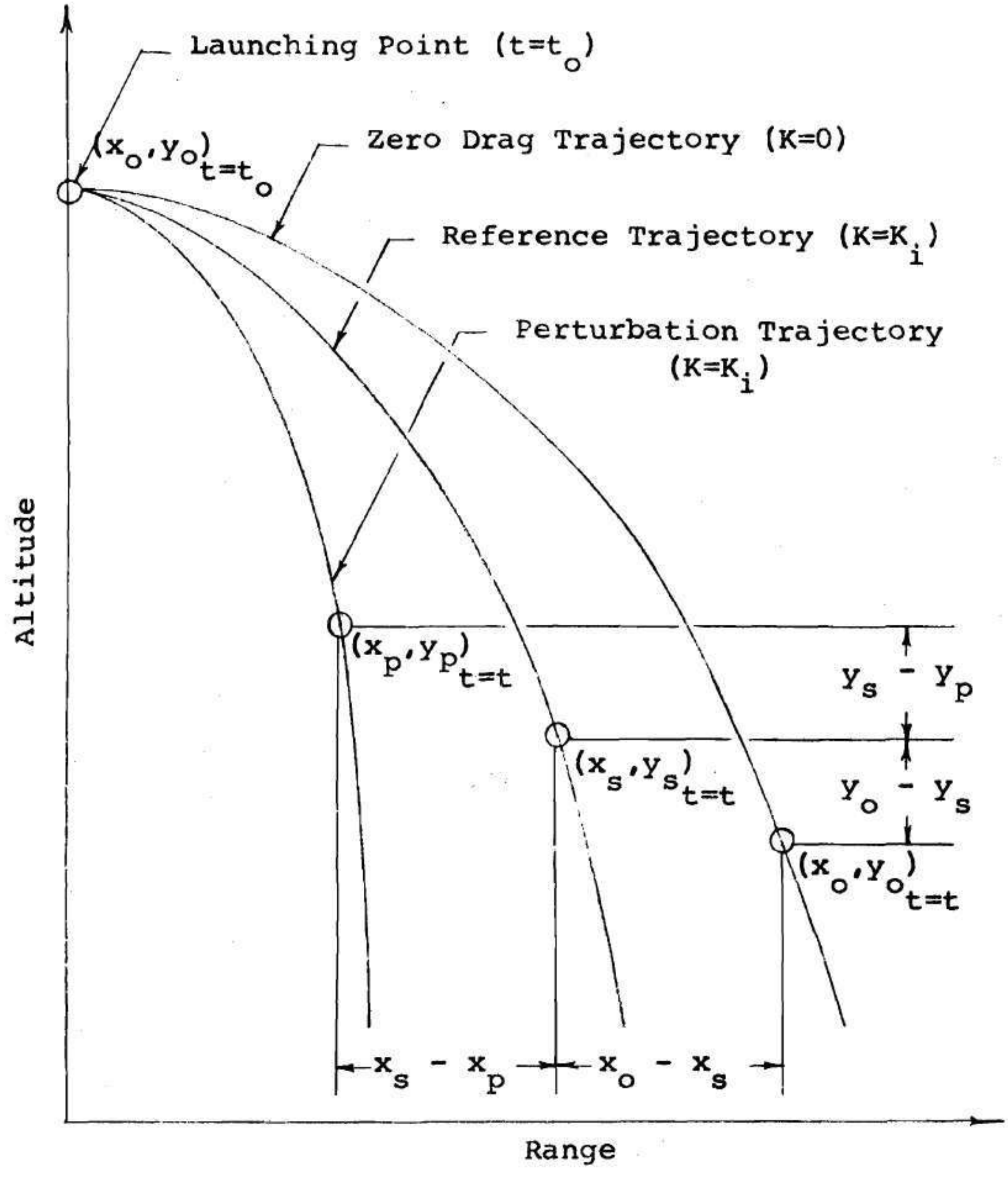

Figure 3. Sketch of the Relationships Between a Zero Drag Trajectory, a Reference Trajectory, and a Perturbation Trajectory.

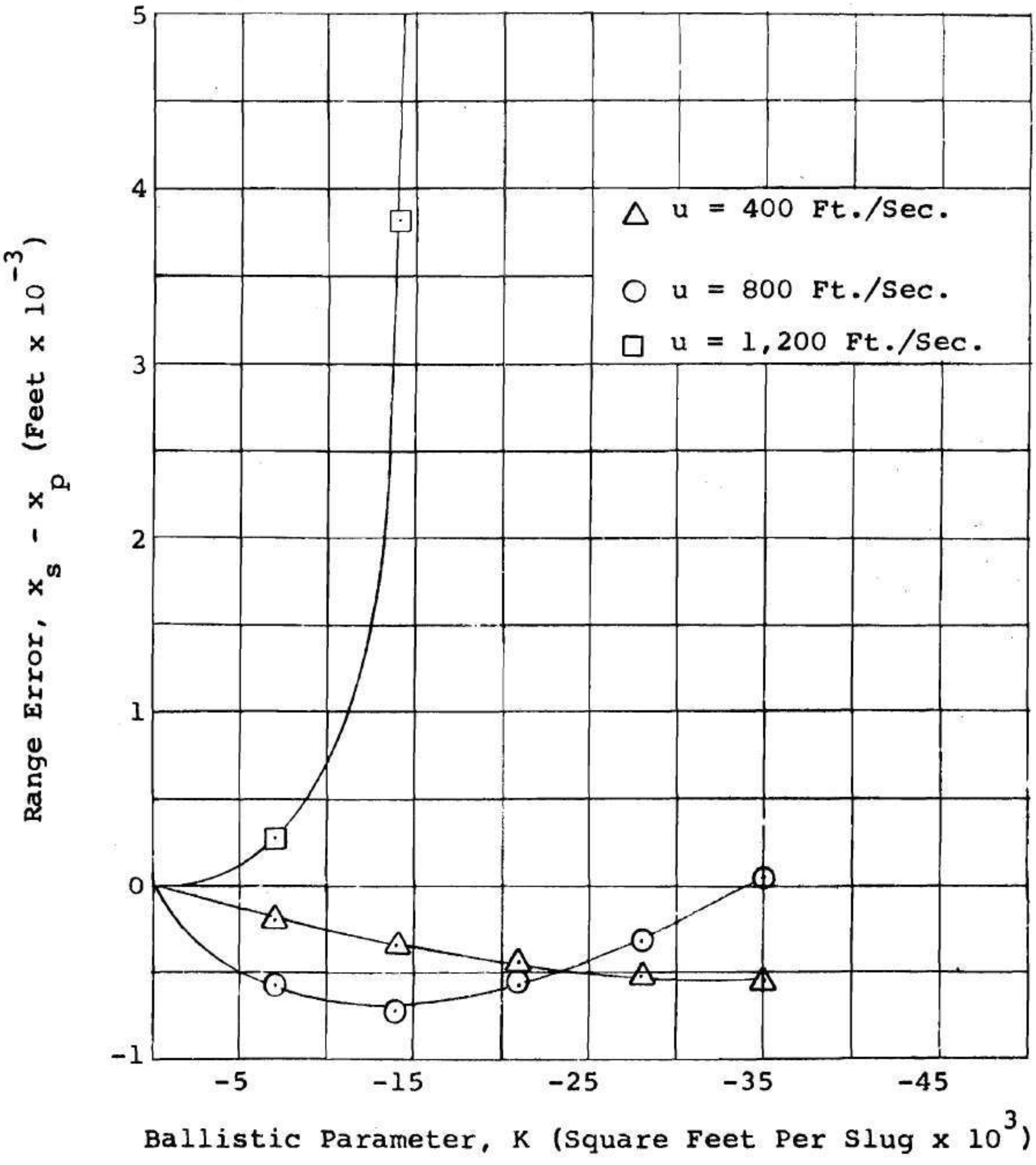

Figure 4. Range Error as a Function of Ballistic Parameter for Initial Conditions of h = 10,000 Feet, u = 400, 800 and 1,200 Feet Per Second.

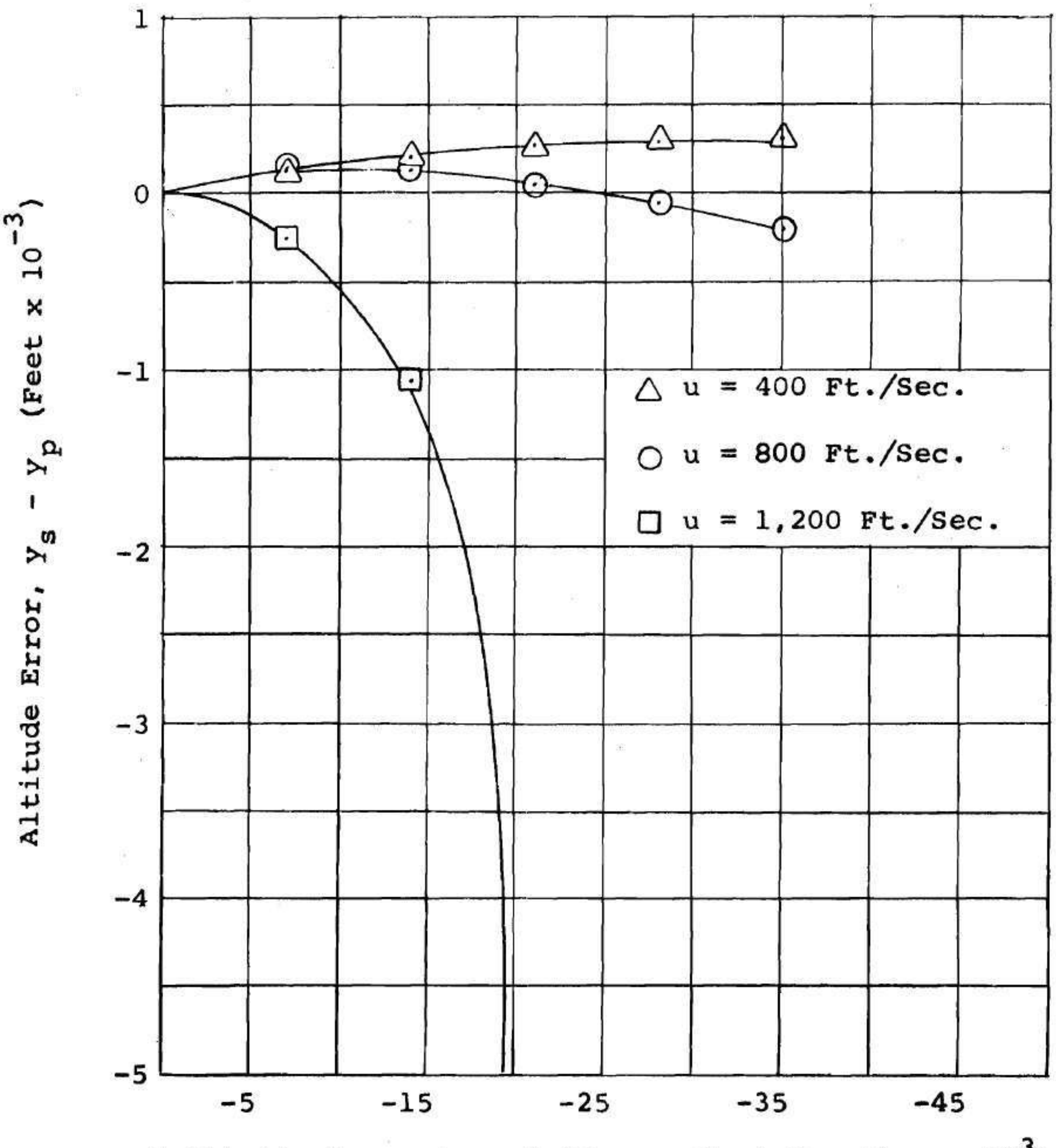

Figure 5. Altitude Error as a Function of Ballistic Parameter for Initial Conditions of h = 10,000 Feet, u = 400, 800 and 1,200 Feet Per Second.

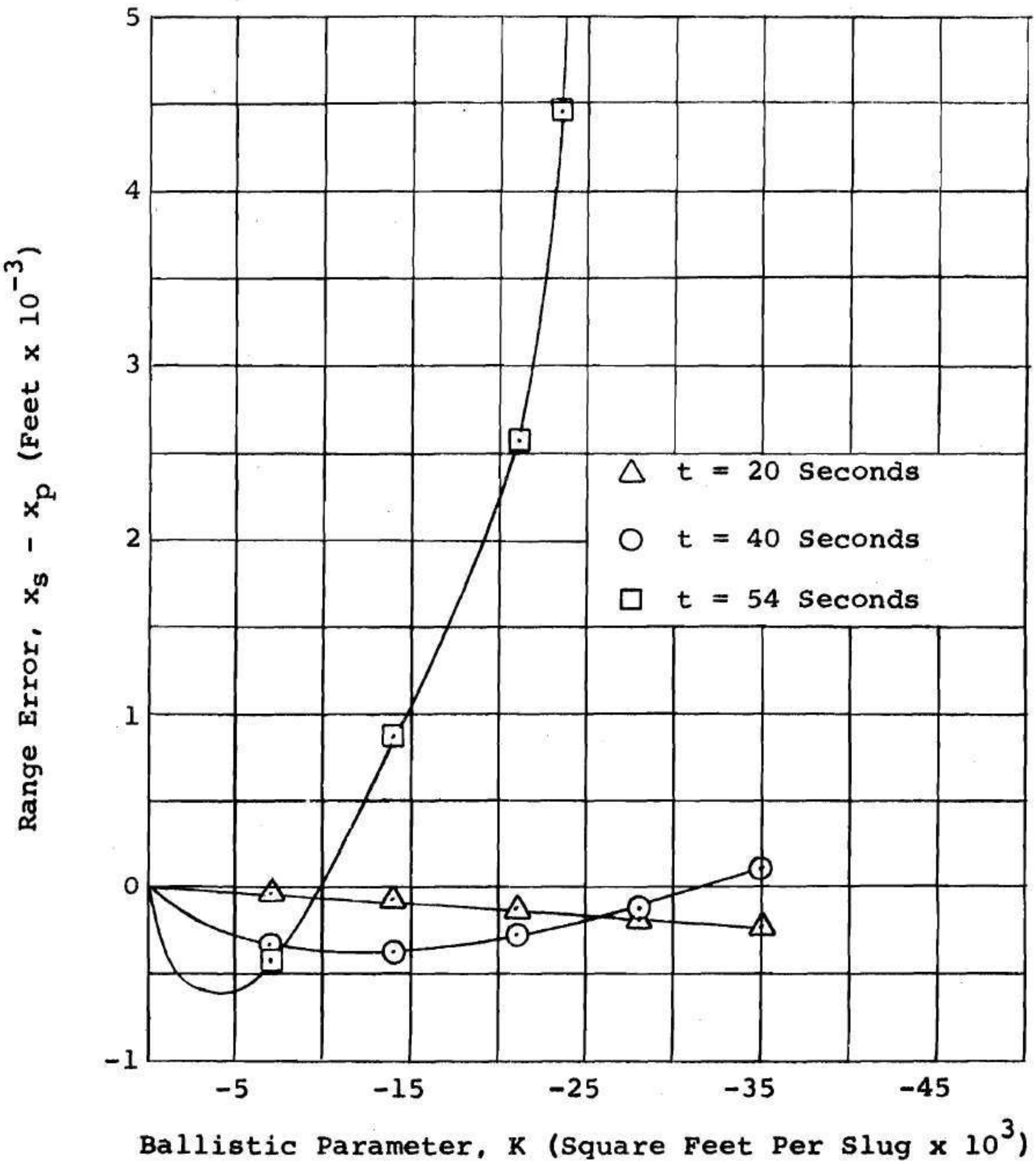

Figure 6. Range Error as a Function of Ballistic Parameter for Initial Conditions of h = 50,000 Feet, u = 400 Feet Per Second.

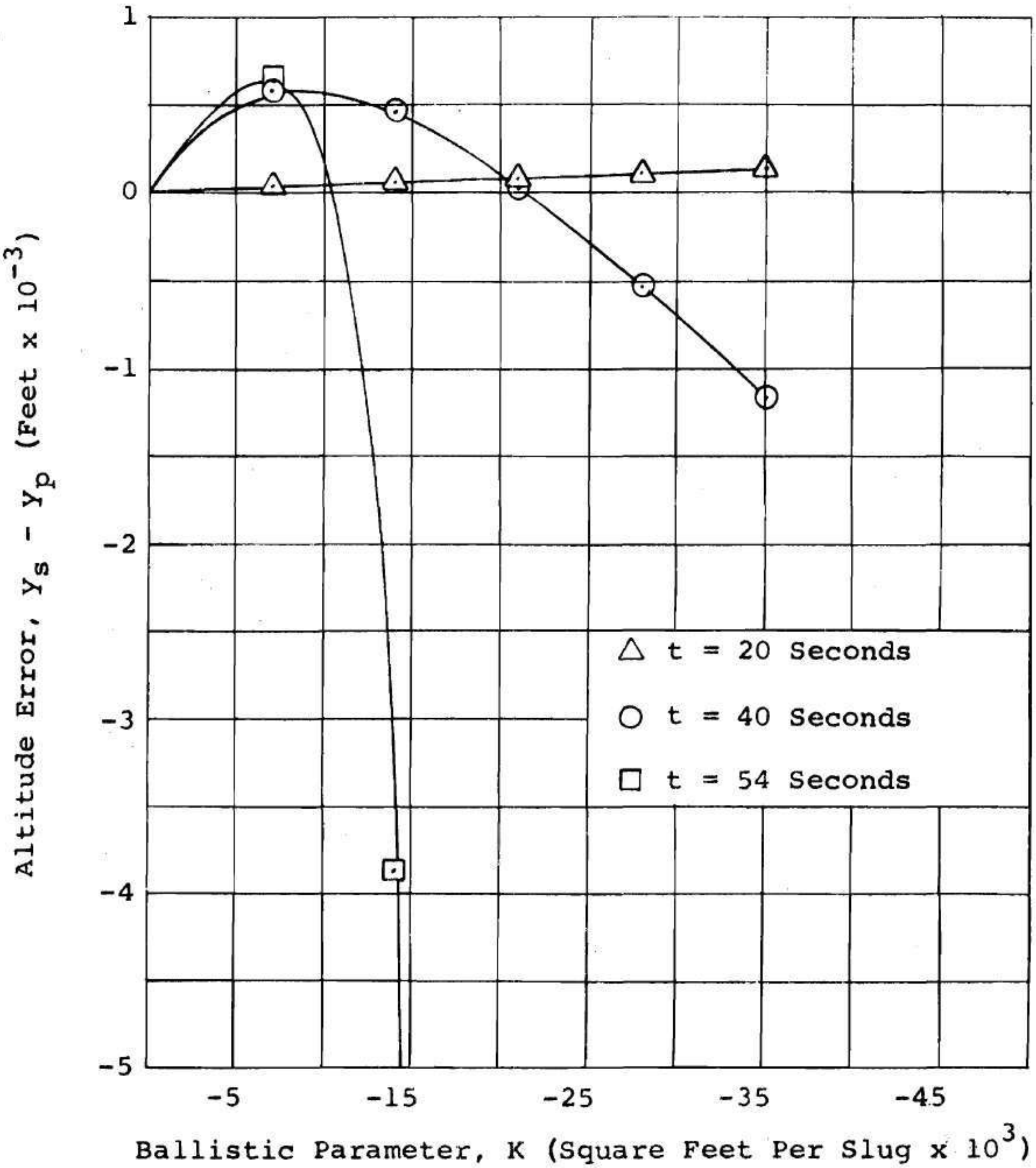

Figure 7. Altitude Error as a Function of Ballistic Parameter for Initial Conditions of h = 50,000 Feet, u = 400 Feet Per Second.

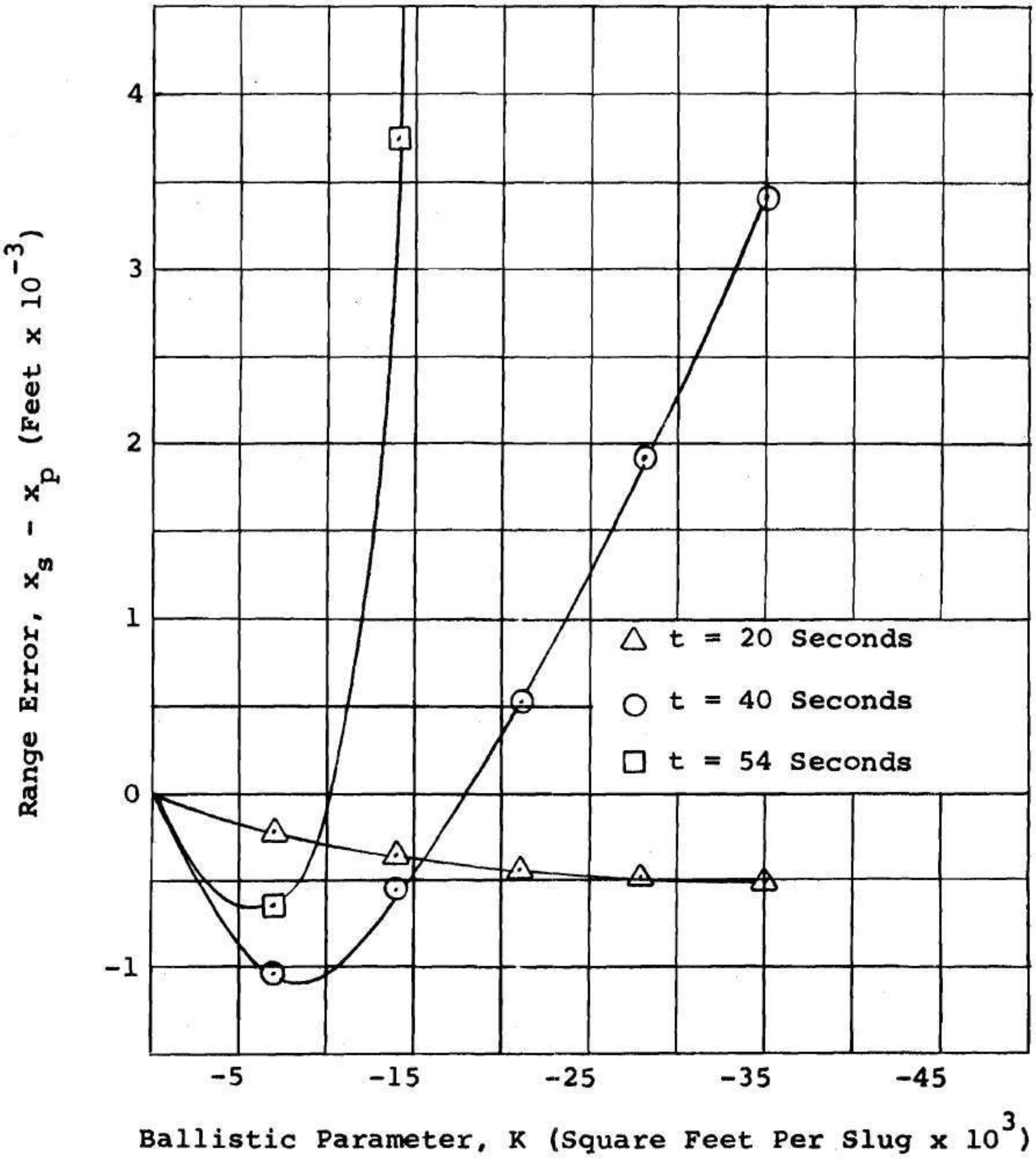

Figure 8. Range Error as a Function of Ballistic Parameter for Initial Conditions of h = 50,000 Feet, u = 800 Feet Per Second.

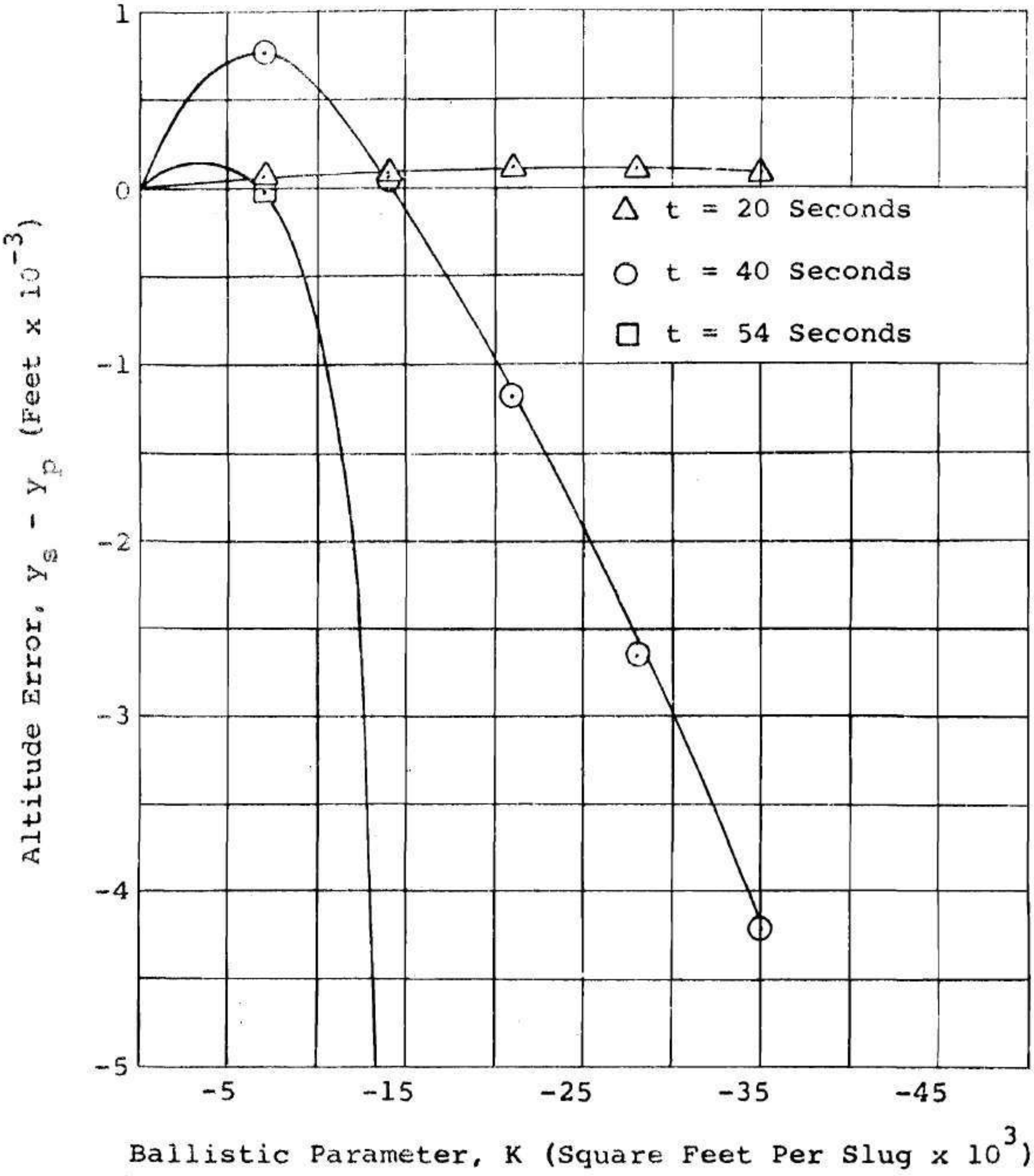

Figure 9. Altitude Error as a Function of Ballistic Parameter for Initial Conditions of h = 50,000 Feet, u = 800 Feet Per Second.

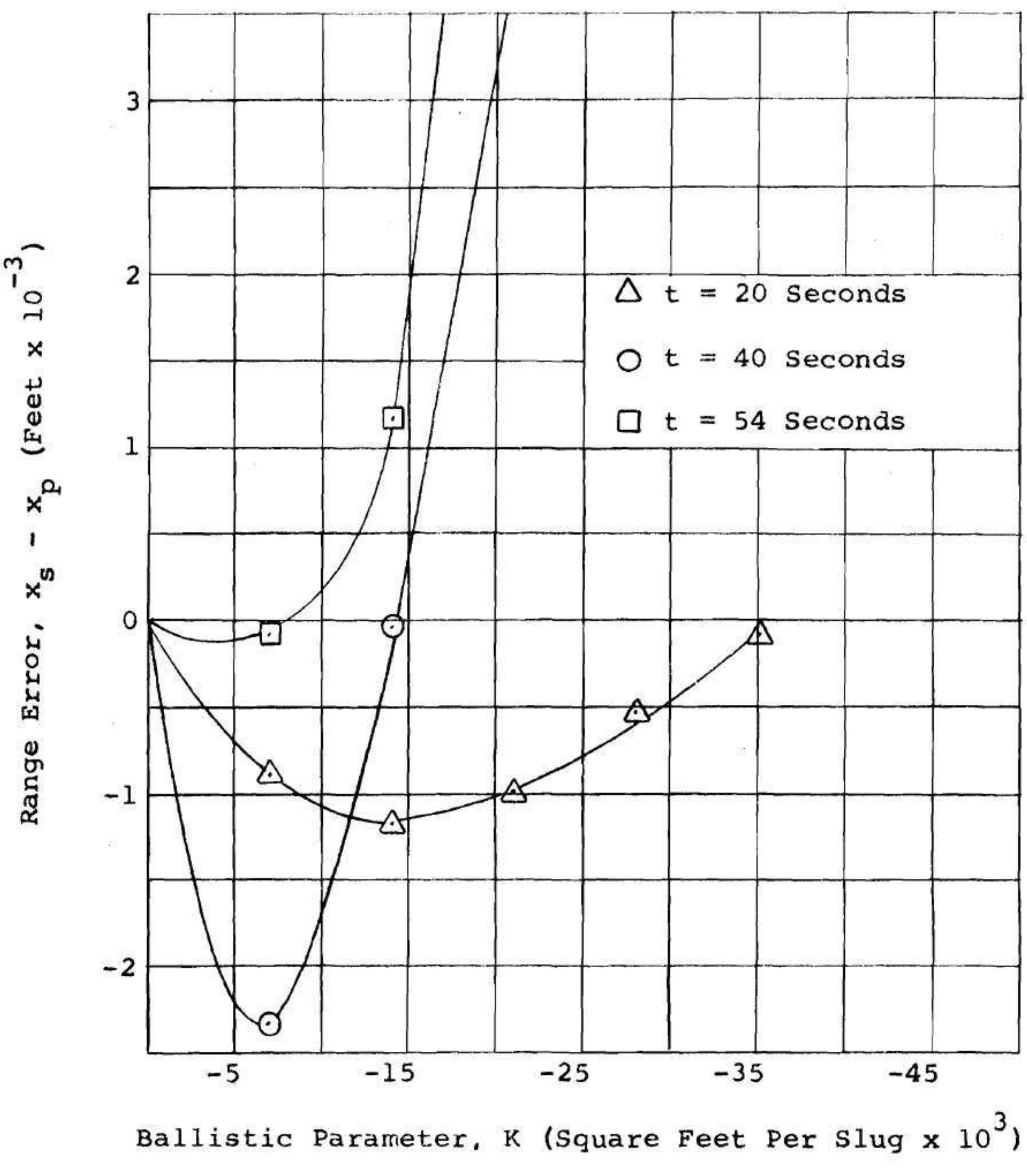

Figure 10. Range Error as a Function of Ballistic Parameter for Initial Conditions of h = 50,000 Feet, u = 1,200 Feet Per Second.

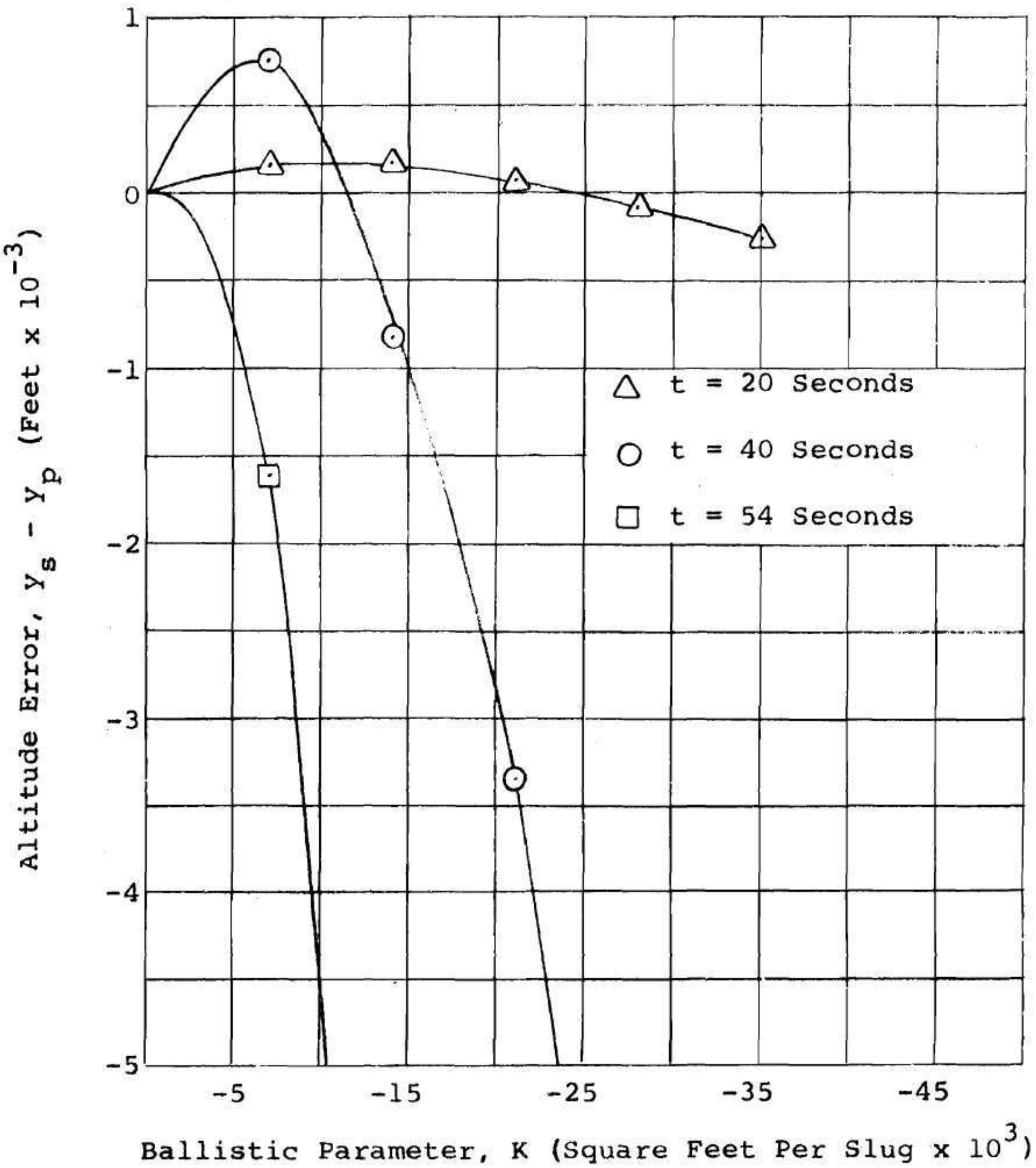

Figure 11. Altitude Error as a Function of Ballistic Parameter for Initial Conditions of $h = 50{,}000$ Feet, $u = 1{,}200$ Feet Per Second.

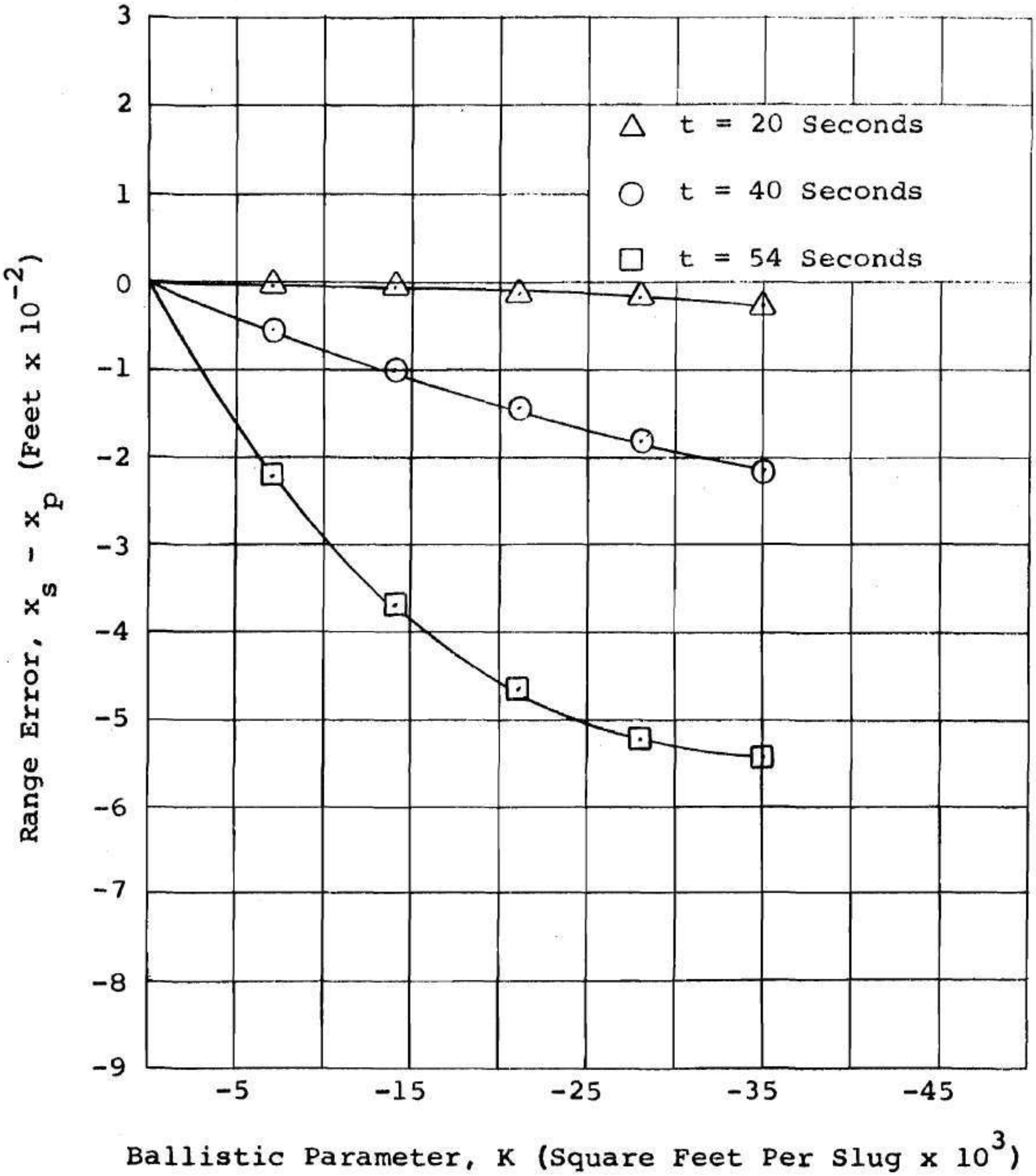

Figure 12. Range Error as a Function of Ballistic Parameter for Initial Conditions of h = 100,000 Feet, u = 400 Feet Per Second.

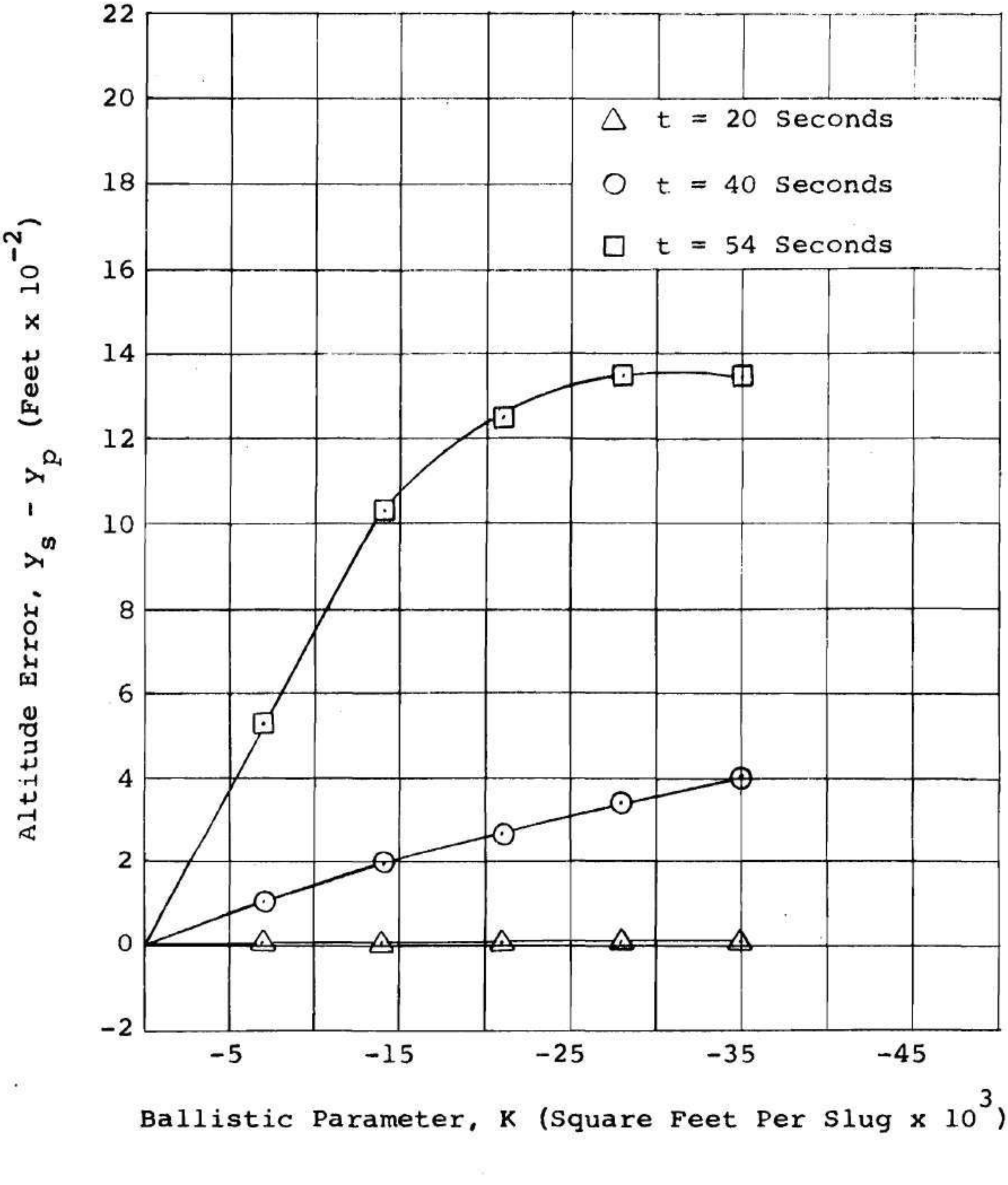

Figure 13. Altitude Error as a Function of Ballistic Parameter for Initial Conditions of h = 100,000 Feet, u = 400 Feet Per Second.

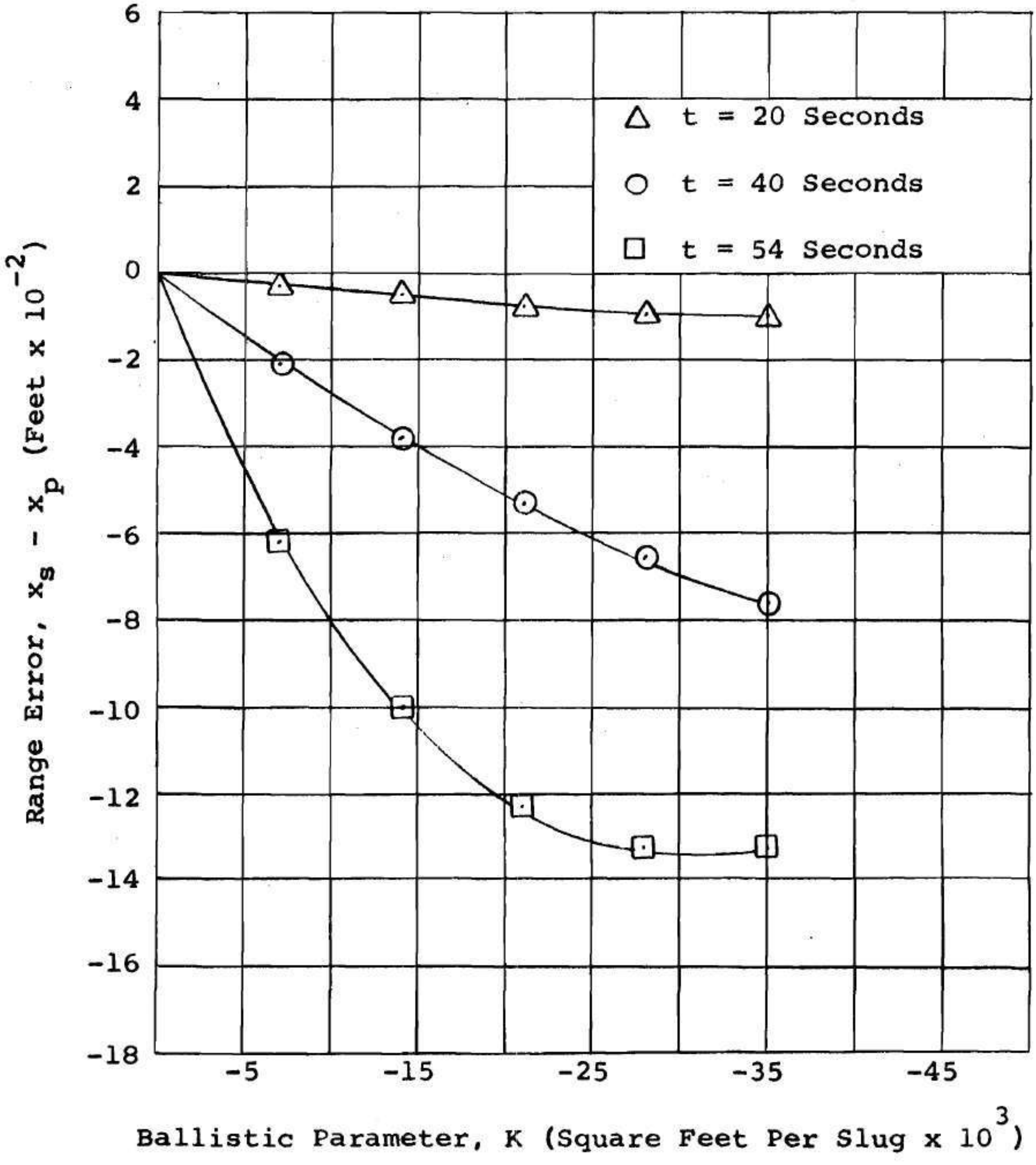

Figure 14. Range Error as a Function of Ballistic Parameter for Initial Conditions of h = 100,000 Feet, u = 800 Feet Per Second.

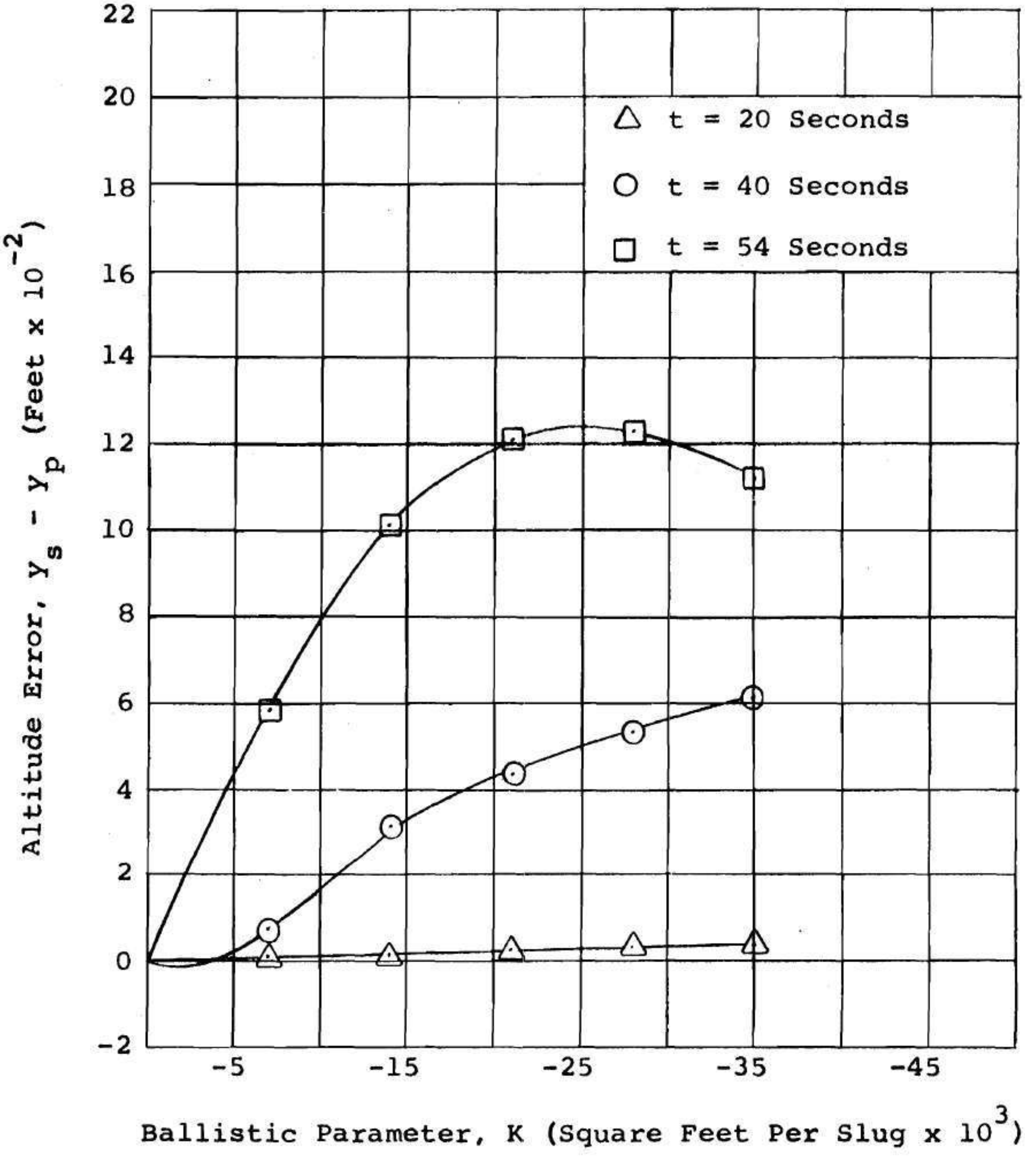

Figure 15. Altitude Error as a Function of Ballistic Parameter for Initial Conditions of h = 100,000 Feet, u = 800 Feet Per Second.

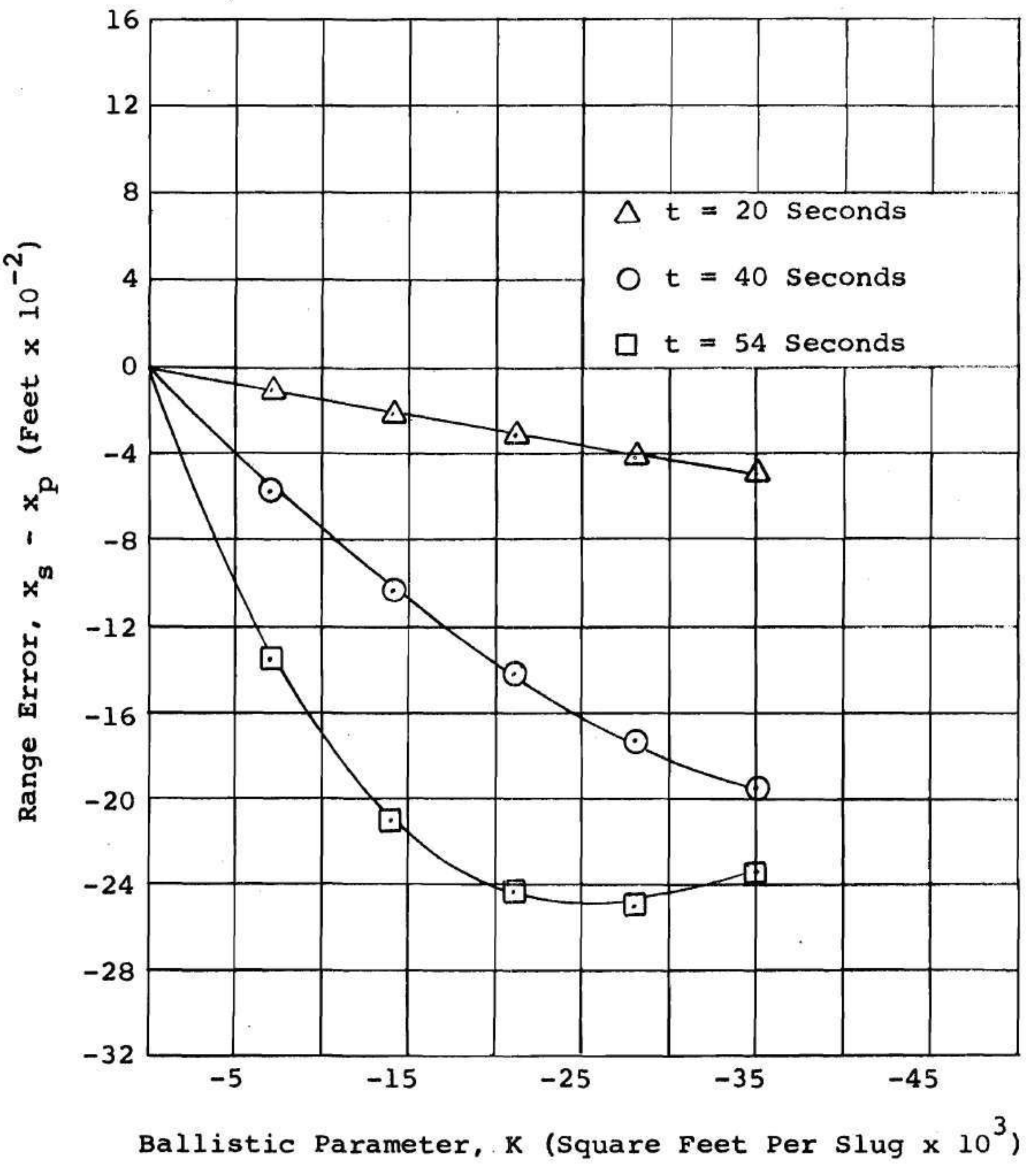

Figure 16. Range Error as a Function of Ballistic Parameter for Initial Conditions of h = 100,000 Feet, u = 1,200 Feet Per Second.

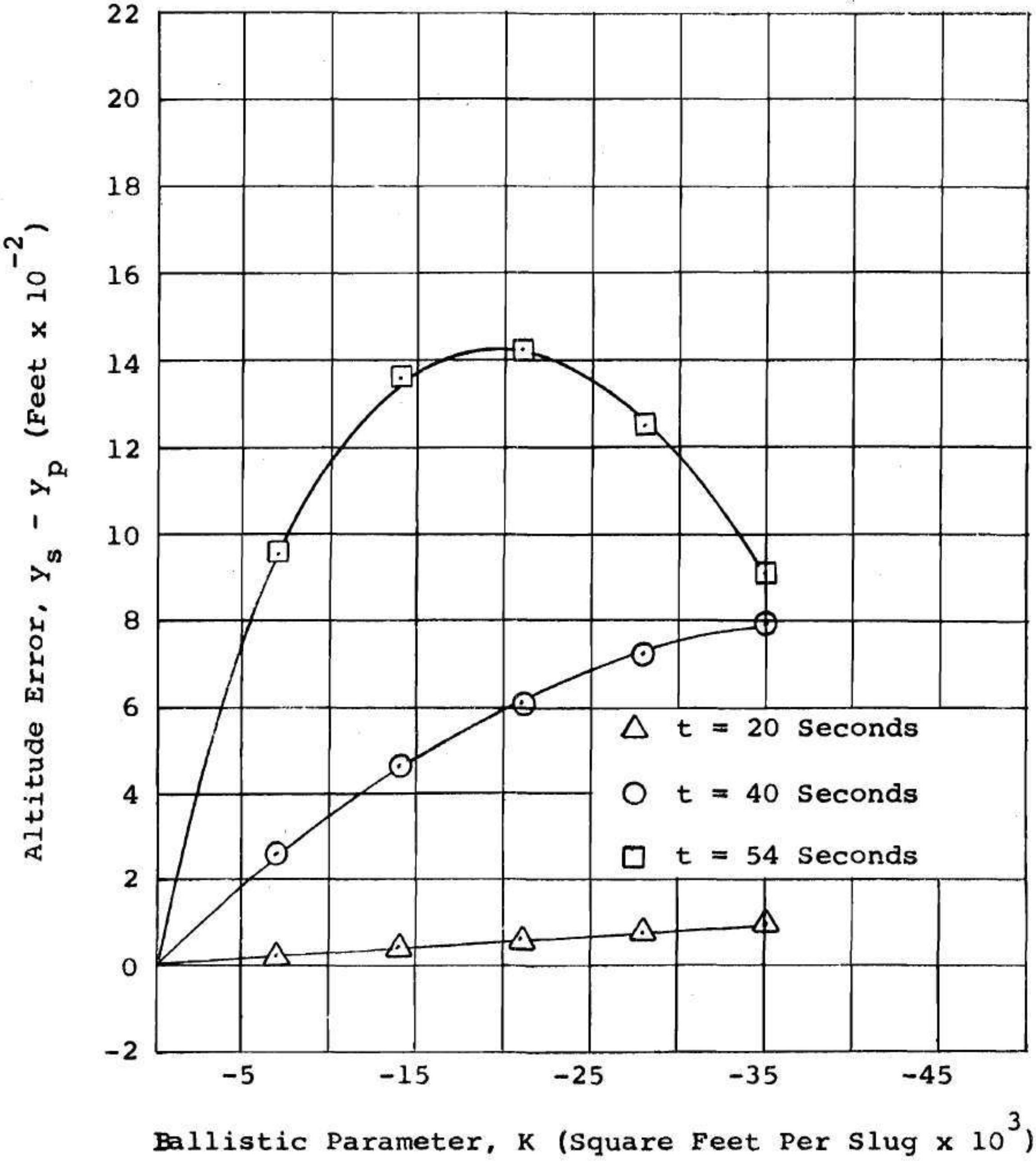

Figure 17. Altitude Error as a Function of Ballistic Parameter for Initial Conditions of h = 100,000 Feet, u = 1,200 Feet Per Second.

Table 2, Range, x_s, and Altitude, y_s, of the Reference Trajectories at $t = 20$ Seconds

Initial Conditions			t = 20 Seconds				
Velocity (Ft./Sec.)	Altitude (Ft.)		-K = 0.007	0.014	0.021	0.028	0.035
400	10,000	range	7,551	7,163	7,822	6,519	6,247
		alt.	3,839	4,072	4,277	4,456	4,616
	50,000	range	7,899	7,802	7,708	7,617	7,529
		alt.	43,629	43,689	43,747	43,803	43,857
	100,000	range	7,991	7,981	7,972	7,963	7,953
		alt.	93,571	93,577	93,583	93,589	93,595
800	10,000	range	14,350	13,183	12,259	11,454	10,777
		alt.	4,031	4,337	4,576	4,792	4,968
	50,000	range	15,499	15,081	14,718	14,391	14,092
		alt.	43,722	43,843	43,943	44,031	44,109
	100,000	range	15,949	15,899	15,851	15,803	15,756
		alt.	93,582	93,598	93,613	93,626	93,643
1,200	10,000	range	18,589	16,444	14,978	13,844	12,900
		alt.	4,383	4,659	4,862	5,033	5,190
	50,000	range	21,827	20,268	19,162	18,345	17,697
		alt.	43,968	44,228	44,380	44,472	44,537
	100,000	range	23,769	23,545	23,327	23,117	22,912
		alt.	93,610	93,652	93,693	93,732	93,770

Table 3. Range, x_s, and Altitude, y_s,

of the Reference Trajectories at t = 40 Seconds

Initial Conditions			t = 40 Seconds				
Velocity (Ft./Sec.)	Altitude (Ft.)	-K =	0.007	0.014	0.021	0.028	0.035
400	50,000	range	15,060	14,429	13,939	13,519	13,142
		alt.	25,994	27,021	27,739	28,322	28,831
	100,000	range	15,892	15,789	15,691	15,597	15,507
		alt.	74,471	74,669	74,856	75,033	75,201
800	50,000	range	28,571	26,666	25,393	24,382	23,510
		alt.	27,038	28,374	29,128	29,675	30,134
	100,000	range	31,574	31,178	30,807	30,459	30,133
		alt.	74,622	74,956	75,264	75,551	75,818
1,200	50,000	range	38,729	34,096	31,512	29,760	28,386
		alt.	28,224	29,849	30,528	30,937	31,268
	100,000	range	46,782	45,673	44,655	43,715	42,842
		alt.	74,822	75,321	75,771	76,179	76,552

Table 4. Range, x_s, and Altitude, y_s, of the Reference Trajectories at t = 54 Seconds

Initial Conditions		t = 54 Seconds					
Velocity (Ft./Sec.)	Altitude (Ft.)	-K =	0.007	0.014	0.021	0.028	0.035
400	50,000	range	18,641	17,382	16,554	15,881	15,297
		alt.	10,924	13,640	15,209	16,426	17,462
	100,000	range	21,111	20,695	20,331	20,008	19,718
		alt.	54,509	55,687	56,700	57,584	58,369
800	50,000	range	34,915	31,704	29,800	28,340	27,107
		alt.	12,799	15,652	17,136	18,222	19,132
	100,000	range	41,799	40,635	39,635	38,757	37,977
		alt.	54,901	56,358	57,577	58,624	59,539
1,200	50,000	range	46,790	40,106	36,655	34,333	32,516
		alt.	14,479	17,556	18,831	19,698	20,428
	100,000	range	61,653	59,119	56,983	55,131	53,493
		alt.	55,416	57,187	58,615	59,809	60,835

Table 5. Configuration of Existing Missiles

Category	Name	Launch Weight W (lbs.)	Body Dia. (Ft.)	Frontal Area S (Ft.Sq.)	W/S	$K = -\frac{g}{2}\frac{C_D S}{W}$
Air-to-Air	Falcon	100	0.5	0.196	511	0.0031
	Sidewinder	155	0.4	0.126	1230	0.0013
Air-to-Surface	Bullpup	600	1.0	0.785	765	0.0021
	Quail	1,100	1.5	1.770	622	0.0026
Anti-Sub.	Able	500	1.0	0.785	640	0.0025
Surface-to-Air	Bomarc	15,000	3.0	7,060	2120	0.0007
	Hawk	1,250	1.2	1.130	1111	0.0014
Surface-to-Surface	Atlas	243,000	10.0	78.500	3100	0.0005
	Jupiter	110,000	8.8	61.000	1800	0.0009
	Redstone	62,000	6.0	28.200	2200	0.0007
	Snark	50,000	15.0	177.000	282	0.0057
	Titan	222,000	10.0	78.500	2830	0.0005
Drones	Kingfisher	7,600	2.0	3.140	2420	0.0006
	Teal	350	0.8	0.503	695	0.0023

$C_{D_{min}}$ value of 0.1 is used in evaluating K.

missiles listed in Table 5 have equally low values of the ballistic parameters and there is no case where the K values are greater than -0.007.

In this study the intermediate values between $K = 0$ and $K = -0.007$ have not been computed. From the derivation of the equations in Chapter II, however, it is apparent that these differences equal zero at $K = 0$ (zero drag conditions). It is, therefore, possible to fair the curves over the ballistic parameter range of $-0.007 \leq K \leq 0$ in Figures 4 through 17 and thus obtain a reasonably good approximation of the actual magnitude of these differences.

The magnitude of the errors over the practical range of ballistic parameters ($-0.007 \leq K \leq 0$) reveals that the perturbation solution to the equations of motion yields trajectories which deviate from the reference trajectories by five per cent or less.

The drag coefficient curve shown in Figure 2 is characteristic of relatively high drag type missiles. The existing missiles and the missiles which are currently under development have considerably lower drag characteristics as also indicated in Table 5. Since the errors, i.e., values of $x_s - x_p$ and $y_s - y_p$ are directly proportional to $\overline{C}_D$ it is felt that even better agreement between the perturbation and reference solutions would be realized if a more realistic $\overline{C}_D$ curve, corresponding to streamlined missiles, were used.

The maximum errors, $x_s - x_p$ (Figure 10) and $y_s - y_p$ (Figure 11), are of the order of two hundred and thirty per cent of the reference range (Tables 2 through 4) and two hundred and five per cent of the reference altitude (Tables 2 through 4), respectively, for the following initial conditions.

$$h = 50{,}000 \text{ feet}$$

$$u = 1{,}200 \text{ feet per second}$$

The ballistic parameter in both cases is -0.035.

A ballistic parameter of K = -0.035 would normally represent a very bluff body; thus such a value of K is not representative of the streamlined missiles which are in service at present.

CHAPTER V

CONCLUSIONS

Within the limitations of the assumptions needed for the derivation of the reference and perturbation equations of motion, the range of the initial altitudes, the initial horizontal velocities, and the ballistic parameters considered, it is concluded that:

1. The perturbation solution to the equations of motion yields trajectories which correlate with the reference trajectories over the ballistic parameter range of $-0.007 \leq K \leq 0$, which includes the values of the ballistic parameters of most existing missiles.

2. Over the ballistic parameter range of $-0.035 \leq K \leq -0.007$ there is very poor correlation between the trajectories.

3. The correlation between the trajectories is also a function of the drag coefficient characteristics. Since existing missiles will in general have lower $\overline{C}_D$ values than those used in this study, a better correlation between the trajectories should be expected if a more realistic $\overline{C}_D$ curve

were used in the computations.

4. The perturbation solution to the equations of motion renders itself as a field method of predicting trajectories of freely falling ballistic missiles since only a comparatively short time of calculations on a hand calculator is required to generate a trajectory having initial conditions of the order used in this study.

CHAPTER VI

RECOMMENDATIONS

It is recommended that:

1. $\overline{C}_D$ characteristics of several different values be used in conjunction with the perturbation solution in order to determine the effect of $\overline{C}_D$ on the correlation of the trajectories.

2. A second perturbation solution to the equations of motion be derived in order to improve the correlation of the trajectories over a larger range of ballistic parameters.

REFERENCES

1. Hutchinson, H. A., *A Study of the Trajectories of a Missile As a Function of Initial Altitude, Initial Horizontal Velocity and Ballistic Coefficient,* Unpublished Master's Thesis, Georgia Institute of Technology, February, 1959.

2. Minzner, R. A., and Riplet, W. S., *The ARDC Model Atmosphere 1956,* Armed Services Technical Information Agency Document 110233.

3. Klein, H., *Some Notes on Dynamics of Trajectories*, Douglas Santa Monica - 23288.

4. Kooy, J. M. J., and Uytenbogaart, J. W. H., *Ballistics of the Future,* Technical Publishing Company, Haarlem, Holland, 1947.

APPENDIX A

EXPANSION OF DENSITY, SPEED OF SOUND, AND DRAG COEFFICIENT IN POWER SERIES OF K

Expanding ρ in power series in y, and y in power series in K, results in:

$$\rho = b_o + b_1 y + b_2 y^2 + b_3 y^3 + \ldots \qquad (1\text{-A})$$

$$y = y_o + y_1 K + y_2 K^2 + y_3 K^3 + \ldots \qquad (2\text{-A})$$

Substituting Equation (2-A) into Equation (1-A) results in:

$$\begin{aligned}\rho = b_o &+ b_1\left[y_o + y_1 K + y_2 K^2 + \ldots\right] + \\ &b_2\left[y_o + y_1 K + y_2 K^2 + \ldots\right]^2 + \\ &b_3\left[y_o + y_1 K + y_2 K^2 + \ldots\right]^3 + \ldots\end{aligned} \qquad (3\text{-A})$$

Separating Equation (3-A) into terms including and excluding K results in:

$$\rho = \left[b_o + b_1 y_o + b_2 y_o^2 + b_3 y^3 + \dots \right] + \qquad (4\text{-A})$$

$$K y_1 \left[b_1 + 2b_2 y_o + {}^{3}{}_{b} y_o^2 + \dots \right] +$$

$$K^2 y_2 \left[b_1 + 2b_2 y_o + 3b_3 y_o^2 + \dots \right] + \dots$$

or

$$\rho = \rho(y_o) + K y_1 \frac{d\rho}{dy}(y_o) + K^2 y_2 \frac{d\rho}{dy}(y_o) + \dots \qquad (5\text{-A})$$

where the symbol ( ) denotes that the variable preceding the parenthesis is a function of the variable within the parenthesis, and the subscript zero denotes zero drag conditions.

Similar to the expansion of the density above, the speed of sound, a, can be expanded and the result is:

$$a = a(y_o) + K y_1 \frac{da}{dy}(y_o) + K^2 y_2 \frac{da}{dy}(y_o) + \dots \qquad (6\text{-A})$$

The non-dimensional drag coefficient, $\overline{C}_D$, can be expanded in power series in Mach number, M, as follows:

$$\overline{C}_D = E_o + E_1 M + E_2 M^2 + E_3 M^3 + E_4 M^4 + \dots \qquad (7\text{-A})$$

Since the drag coefficient is an even function of Mach number, Equation (7-A) can be written as:

$$\overline{C}_D = E_o + E_2 M^2 + E_4 M^4 + \dots \qquad (8\text{-A})$$

Expanding M in a power series in K results in:

$$M = M_o + M_2K^2 + M_4K^4 + \ldots \qquad (9\text{-}A)$$

Substituting Equation (9-A) into Equation (8-A) results in:

$$\bar{C}_D = E_o + E_2\left[M_o + M_2K^2 + M_4K^4 + \ldots\right]^2 + \qquad (10\text{-}A)$$
$$E_4\left[M_o + M_2K^2 + M_4K^4 + \ldots\right]^4 + \ldots$$

Separating Equation (10-A) into terms including and excluding K results in:

$$\bar{C}_D = \left[E_o + E_2M_o^2 + E_4M_o^4 + \ldots\right] + \qquad (11\text{-}A)$$
$$2K^2M_2\left[E_2M_o + 2E_4M_o^3 + \ldots\right] +$$
$$2K^4M_4\left[E_4M_o + 2E_4M_o^3 + \ldots\right] + \ldots$$

or $$\bar{C}_D = \bar{C}_D(M_o) + K^2\left[2E_2M_oM_2 + 4E_4M_o^3M_2 + \ldots\right] + \qquad (12\text{-}A)$$
$$K^4\left[2E_2M_oM_4 + 4E_4M_o^3M_4 + \ldots\right] + \ldots$$

By definition:

$$M = \frac{V}{a} \qquad (13\text{-}A)$$

Substitution of Equations (12), (29) and (32) in Chapter II into Equation (13-A) results in:

$$M = \frac{\left[u^2 + g^2t^2 + 2K\ ux_1' - gt\ y_1' + \dots\right]^{0.5}}{a(y_o) + Ky_1 \frac{da}{dy}(y_o) + K^2 y_2 \frac{da}{dy}(y_o) + \dots} \qquad (14\text{-A})$$

After long division of the right hand term, it is possible to rewrite Equation (14-A) in the following form:

$$M = \left\{ \frac{u^2 + g^2t^2}{\left[a(y_o)\right]^2} + \frac{2K\left[ux_1' - gt\ y_1'\right] + \dots}{\left[a(y_o)\right]^2} + \right. \qquad (15\text{-A})$$

$$\left. \frac{2K\left[ux_1' - gt\ y_1'\right] - \dfrac{\left[2a(y_o)\ Ky_1 \frac{da}{dy}(y_o)\right]\left[u^2 + g^2t^2\right]}{a(y_o)^2}}{\left[a(y_o)\right]^2 + 2a(y_o)\ Ky_1 \frac{da}{dy}(y_o) + 2a(y_o)\ K^2y_2 \frac{da}{dy}(y_o) + \dots} \right\}^{0.5}$$

Substitution of Equation (15-A) into Equation (12-A) results in:

$$\bar{C}_D = \bar{C}_D \left\{ \frac{u^2 + g^2t^2}{\left[a(y_o)\right]^2} + \frac{2K\left[ux_1' - gt\ y_1'\right] + \dots}{\left[a(y_o)\right]^2} + \right. \qquad (16\text{-A})$$

$$\left. \frac{2K\left[ux_1' - gt\ y_1'\right] - \dfrac{\left[2a(y_o)\ Ky_1 \frac{da}{dy}(y_o)\right]\left[u^2 + g^2t^2\right]}{\left[a(y_o)\right]^2}}{\left[a(y_o)\right]^2 + 2a(y_o)\ Ky_1 \frac{da}{dy}(y_o) + 2a(y_o)\ K^2y_2 \frac{da}{dy}(y_o) + \dots} \right\}^{0.5} +$$

$$K^2\left[2E_2M_oM_2 + 4E_4M_o^3M_2 + \dots\right] +$$

$$K^4\left[2E_2M_oM_4 + 4E_4M_o^3M_4 + \dots\right] + \dots$$

Substituting Equations (28) through (33) in Chapter II and Equations (5-A) and (16-A) into Equations (17) and (18) in Chapter II results in:

$$Kx_1'' + K^2 x''_2 = K \left\{ \bar{C}_D \left\{ \frac{u^2 + g^2t^2}{\left[a(y_o)\right]^2} + \frac{2K\left[ux_1' - gt\, y_1'\right] + \ldots}{\left[a(y_o)\right]^2} + \right.\right. \tag{17-A}$$

$$\left. \frac{2K\left[ux_1' - gt\, y_1'\right] - \dfrac{\left[2a(y_o)\, Ky_1 \frac{da}{dy}(y_o)\right]\left[u^2 + g^2t^2\right]}{\left[a(y_o)\right]^2}}{\left[a(y_o)\right]^2 + 2a(y_o)\, Ky_1 \frac{da}{dy}(y_o) + 2a(y_o)\, K^2y_2 \frac{da}{dy}(y_o) + \ldots} \right\}^{0.5} +$$

$$K^2\left[2E_2M_oM_2 + 4E_4M_o^3M_2 + \ldots\right] +$$

$$\left. K^4\left[2E_2M_oM_4 + 4E_4M_o^3M_4 + \ldots\right] + \ldots \right\}$$

$$\left[\rho\,(y_o) + Ky_1 \frac{d\rho}{dy}(y_o) + K^2y_2 \frac{d\rho}{dy}(y_o) + \ldots\right]$$

$$\left[u^2 + g^2t^2 + 2K\left[ux_1' - gt\, y_1'\right] + \ldots\right]$$

$$\left[u + Kx_1' + K^2x_2' + \ldots\right]$$

and

$$
\begin{aligned}
-g + Ky_1'' + K^2 y_2'' = K \Bigg\{ \bar{C}_D \Bigg\{ & \frac{u^2 + g^2 t^2}{\left[a(y_o)\right]^2} + \frac{2K\left[ux_1' - gt\ y_1'\right] + \dots}{\left[a(y_o)\right]^2} + \qquad (18\text{-A}) \\
& \left. \frac{2K\left[ux_1' - gt\ y_1'\right] - \dfrac{\left[2a(y_o)\ Ky_1 \frac{da}{dy}(y_o)\right]\left[u^2 + g^2 t^2\right]}{\left[a(y_o)\right]^2}}{\left[a(y_o)\right]^2 + 2a(y_o)\ Ky_1 \frac{da}{dy}(y_o) + 2a(y_o)\ K^2 y_2 \frac{da}{dy}(y_o) + \dots} \right\}^{0.5} + \\
& K^2\left[2E_2 M_o M_2 + 4E_4 M_o^3 M_2 + \dots\right] + \\
& K^4\left[2E_2 M_o M_4 + 4E_4 M_o^3 M^4 + \dots\right] + \dots \Bigg\} \\
& \left[\rho\ (y_o) + Ky_1 \frac{d\rho}{dy}(y_o) + K^2 y_2 \frac{d\rho}{dy}(y_o) + \dots\right] \\
& \left[u^2 + g^2 t^2 + 2K\left[ux_1' - gt\ y_1'\right] + \dots\right] \\
& \left[-gt + Ky_1' + K^2 y_2'\right] - g
\end{aligned}
$$

The object is to retain only first perturbation terms, i.e., terms involving only the first power of K. K, however, cancels on both sides of Equations (17-A) and (18-A). Thus, in effect, only terms which do not contain K at all are being kept. Equations (17-A) and (18-A) can now be written as follows:

$$x''_1 = K\bar{C}_D \left[\frac{\left[u^2 + g^2t^2\right]^{0.5}}{a(y_o)} \right] \rho\ (y_o) \left[u^2 + g^2t^2\right]^{0.5} \left[u\right] \quad (19\text{-A})$$

$$y''_1 = -K\bar{C}_D \left[\frac{\left[u^2 + g^2t^2\right]^{0.5}}{a(y_o)} \right] \rho\ (y_o) \left[u^2 + g^2t^2\right]^{0.5} \left[gt\right] \quad (20\text{-A})$$

APPENDIX B

RELATIONS FOR DENSITY AND SPEED OF SOUND

The following curve fits are consistent with those used by Hutchinson in Reference 1 and those used by the Sandia Corporation.

<u>Altitudes Up to 35,332 Feet</u>.--

Density $\rho = 0.002378 \left[(145{,}366 - y)/145{,}366\right]^{4.255}$

Speed of Sound $c = 1117.0 \left[(145{,}366 - y)/145{,}366\right]^{0.5}$

<u>Altitudes Between 35,332 Feet and 104,987 Feet</u>.--

Density $\rho = 0.00314158 \left[10^{\,((4705 - y)/48{,}211)}\right]$

Speed of Sound $c = 971.0$

Density has the units of slugs per cubic feet and speed of sound has the units of feet per second.

APPENDIX C

RELATIONS BETWEEN DRAG COEFFICIENT AND MACH NUMBER

The following curve fit expressions are consistent with those used by the Sandia Corporation.

At $M \leq M_o$ $\quad C_D = 1.0$

At $M_o < M \leq M_1$ $\quad C_D = A_1 + B_1 \, (M)$

At $M_1 < M < M_2$ $\quad C_D = A_2 + B_2 \tan^{-1} C_2 \, (M - D_2)$

At $M \geq M_2$ $\quad C_D = A_3 + B_3 \, (M)$

where:

$M_o = 0.5$ $\qquad A_3 = 1.9307$

$M_1 = 0.61$ $\qquad B_1 = 0.140$

$M_2 = 1.3$ $\qquad B_2 = 0.92652937$

$A_1 = 0.93$ $\qquad B_3 = 1.0433$

$A_2 = 2.1493365$ $\qquad C_2 = 8.4771050$

$D_2 = 0.96944160$